

# Analyst

Accepted Manuscript

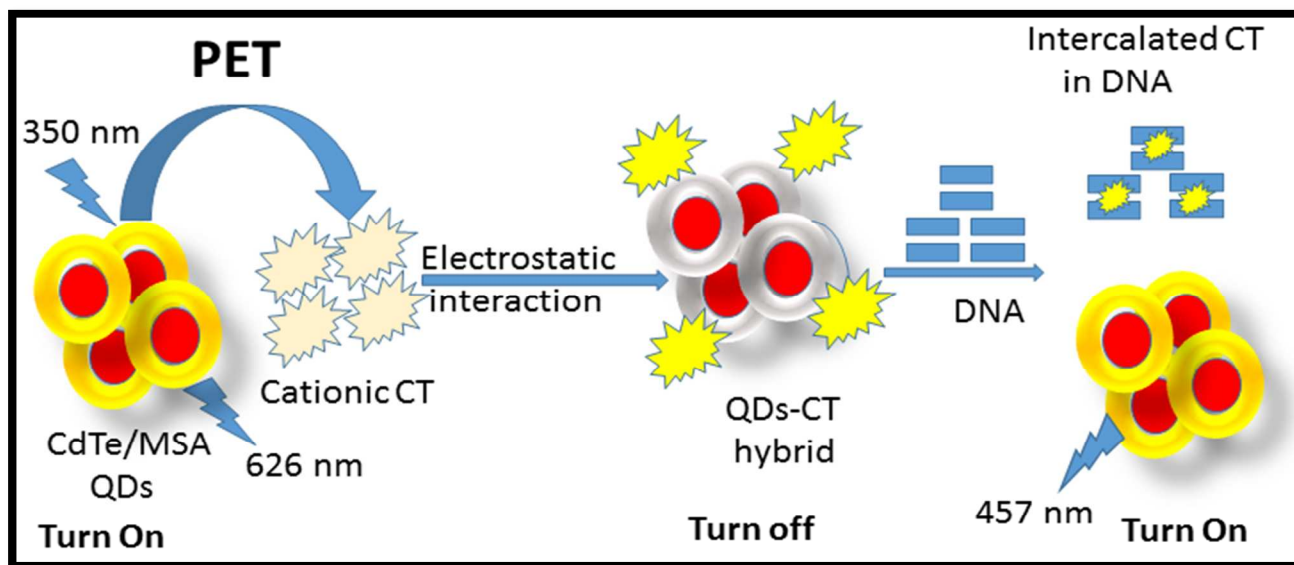


This is an *Accepted Manuscript*, which has been through the Royal Society of Chemistry peer review process and has been accepted for publication.

*Accepted Manuscripts* are published online shortly after acceptance, before technical editing, formatting and proof reading. Using this free service, authors can make their results available to the community, in citable form, before we publish the edited article. We will replace this *Accepted Manuscript* with the edited and formatted *Advance Article* as soon as it is available.

You can find more information about *Accepted Manuscripts* in the [Information for Authors](#).

Please note that technical editing may introduce minor changes to the text and/or graphics, which may alter content. The journal's standard [Terms & Conditions](#) and the [Ethical guidelines](#) still apply. In no event shall the Royal Society of Chemistry be held responsible for any errors or omissions in this *Accepted Manuscript* or any consequences arising from the use of any information it contains.



'Turn on-off-on' sensor for highly sensitive detection of ds DNA with excellent 'Limit of Detection'.

# Supramolecular nanobiological hybrid as a PET sensor for bacterial DNA isolated from *Streptomyces sanglieri*

Sudesna Chakravarty<sup>1</sup>, Dilip Saikia<sup>2</sup>, Priyanka Sharma<sup>3</sup>, Nirab Chandra Adhikary<sup>4</sup>, Debajit Thakur<sup>5</sup> and Neelotpal Sen Sarma<sup>6\*</sup>

1, 6\*: Polymer Laboratory, Physical Sciences Division, Institute of Advanced Study in Science and Technology, Guwahati-781035, India

2, 4: Plasma Section, Physical Sciences Division, Institute of Advanced Study in Science and Technology, Guwahati-781035, India

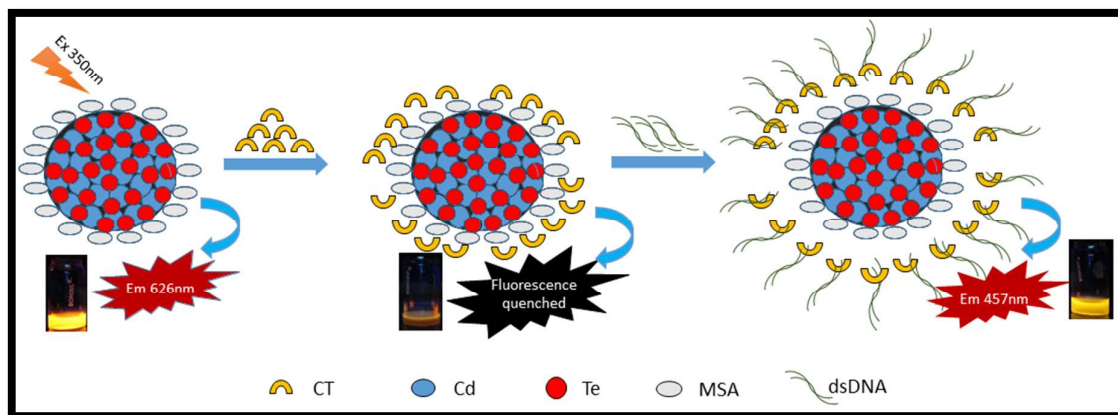
3, 5: Microbial Biotechnology Laboratory, Life Sciences Division, Institute of Advanced Study in Science and Technology, Guwahati-781035, India

**Abstract:** Development of rapid, label free, cost effective and highly efficient sensor for DNA detection is of great importance in disease diagnosis. Herein, we have reported a new hybrid fluorescent probe based on cationic curcumin-tryptophan complex and water soluble mercapto succinic acid (MSA) capped CdTe quantum dots (QDs) for the detection of double stranded DNA (ds DNA) molecules. Cationic curcumin-tryptophan complex (CT) directly interacts with negatively charged MSA capped quantum dots via electrostatic coordination, resulting in Photoluminescence (PL) quenching of QDs via Photoinduced Electron Transfer (PET) process. Further, addition of ds DNA results in restoration of PL, as CT would intercalate between DNA strands. Thus, this process can be utilized for selective sensing of ds DNA via fluorescence measurements. Under optimized experimental conditions, the PL quenching efficiency of QDs is found to be 99.4% in presence of  $0.31 \times 10^{-9}$  M CT. Interestingly, the regain in PL intensity of QDs-CT is found to be 99.28% in presence of  $1 \times 10^{-8}$  M ds DNA. The detection limit for ds DNA with the sensing probe developed is  $1.4 \times 10^{-10}$  M. Furthermore, the probe is found to be highly sensitive towards bacterial DNA isolated from *Streptomyces sanglieri* with a detection limit of  $1.7 \times 10^{-6}$  M. The present work will provide a new insight to prepare bio inspired hybrid materials as an efficient sensor for disease diagnosis and agricultural development.

**Key words:** Curcumin, tryptophan, PET, ds DNA, CdTe Quantum dots.

**Introduction:** The design of simple, rapid, sensitive and cost effective fluorescent probes for DNA detection plays a vital role in clinical diagnosis, preventive care and drug discovery.<sup>1</sup> Such probes are based on small molecule-DNA interactions including electrostatic interaction or intercalation or groove binding.<sup>2-4</sup> Previously, organic fluorophores were used as probes for DNA sensing. However, traditional fluorescent probes suffer from certain limitations such as long term photostability, short PL lifetime, wide PL spectra and solubility. So, organic fluorescent probes can be merged with highly luminescent semiconductor QDs for superior properties. Such QDs are nanocrystals exhibiting unique optical properties like tunable emission spectra, improved brightness, superior photostability and simultaneous excitation of multiple fluorescence colours.<sup>5, 6</sup> There are many strategies available for DNA detection. Fluorescence Resonance Energy Transfer (FRET) represents one of the most widely used tool for DNA detection in a homogeneous solution.<sup>7, 8</sup> But, this requires dual labelling of the probe molecule with two spectroscopic-distinguishable fluorophores or a fluorophore-quencher pair, which is time consuming, expensive and have poor detection limits.<sup>9-14</sup> But for such purposes, photoinduced electron transfer (PET) process is advantageous. However, there are only few reports available which explain the significance of electron transfer mechanism.<sup>15</sup> Raymo *et.al.* developed a photoinduced electron transfer (PET) based sensor to signal receptor-substrate interactions. Also, Vaishnavi *et.al.* has reported a PET based sensor using quantum dots-cationic porphyrin nanohybrid.<sup>16, 17</sup>

In our present work, we have reported a highly efficient label free sensor for ds DNA using cationic curcumin-tryptophan (CT) and MSA capped CdTe QDs, thus merging together the properties of both organic and inorganic materials. Also, the sensing of bacterial DNA isolated from *Streptomyces sanglieri* with our probe has been studied. CT has been synthesized by covalently linking amino acid tryptophan through their carboxyl function to the phenolic hydroxyl in the two phenyl rings of curcumin where two free amino groups can be generated at two sites. The amino groups are then protonated to generate positively charged CT. Also, to the best of our knowledge, there is no reported work employing cationic CT and QDs as a PET based nano biosensor for sensing ds DNA. The sensor is capable of direct detection of ds DNA without making any chemical modification of the probe with excellent detection limit. Here, the detection of ds DNA depends upon hybrid formation of CT with negatively charged ds DNA. The gradual addition of ds DNA to QD-CT hybrid results in the detachment of QDs from CT surface and subsequent binding of the resultant CT with ds DNA. The reason behind new hybrid formation can be explained from the fact that derivatives of curcumin (curcumin bio-conjugates) can interact with ds DNA by combination of positive (hydrogen bonding, vander waal's and electrostatic) and negative (steric repulsion) interactions.<sup>18</sup> The present strategy of sensing ds DNA is illustrated in the Scheme1 as shown below:



Scheme 1: Sensing strategy for dsDNA

**Materials:** [Curcumin, phenol] (SIGMA), [BOC-L-Tryptophan (SRL), [DNA (degraded free acid ex herring sperm, hs DNA)] (SRL), [Hydrochloric acid Cadmium chloride, ethanol, Sodium Borohydride] (Merck), [Mercapto succinic acid, Sodium Telluride, P-Toluene sulfonic acid] (Loba Chemie), [Citric acid, Borax powder] (Fischer Scientific), [Tris HCl, EDTA, sodium chloride, RNase, Sodium dodecyl sulphate, Proteinase K, chloroform, isoamylalcohol, sodium acetate, Yeast, Malt, Peptone and Starch] (HIMEDIA) .

#### Methods:

**FTIR measurements:** The FTIR spectra were recorded with the help of NICOLET 6700 FTIR spectrophotometer with 32 scans. The sample was prepared under high pressure and subsequently captured in KBr matrix in the form of pellet using standard ratio of Sample: KBr.

**DLS Measurements:** Room temperature zeta potential of the solutions were measured in Malvern Nano ZS90 in a glass cuvette with square aperture with zeta dip cell electrode. Hydrodynamic radius of the particles were also measured in glass cuvette with square aperture.

#### TEM, AFM and XRD characterization:

**TEM characterization:** A few drops of QDs sample were dispersed into a 3 mm copper grid covered with a continuous carbon film and dried at room temperature. TEM characterization was performed on a JEOL JEM 2100 transmission electron microscope operating at 200 kV.

**AFM characterization:** The nature of the surface microstructures was studied using NT-MDT NTEGRA atomic force microscopy (AFM) operated in semi contact mode. The samples were prepared by spin coating in glass slides of dimension 1 cm $\times$ 1 cm.

**XRD characterization:** Crystalline structures of the QDs were identified by powder X-ray diffraction. XRD patterns were obtained using a Bruker D 8 Advance X-ray diffractometer with Cu K $\alpha$  radiation,  $\lambda=0.154$  nm and a Ni filter. The tube current was 40 mA with a tube voltage of 40 kV. The angular range was  $2\theta=10-90^\circ$ .

**Spectroscopic experiments (UV-Vis and PL study):** Room temperature UV-Vis spectra were recorded using UV-Visible spectrophotometer. The fluorescence studies were done using Cary Eclipse spectrophotometer with a halogen lamp as the excitation source, at a scan speed of 240 nm s $^{-1}$ . The excitation and emission slit widths were maintained at 5 nm and the scan rate was kept constant for all the experiments. The detector voltage was maintained at 550 V. Quartz cells (4 $\times$ 1 $\times$ 1 cm) with high vacuum Teflon stopcocks were used for spectral measurements.

**Cyclic Voltammetry (CV) experiments:** The CV measurements were performed on a CH instruments electrochemical workstation, with a typical three-electrode system consisting of glassy carbon working electrode, Ag/Ag $^+$  reference electrode and a platinum wire counter electrode with 0.5 M KCl in water as an electrolyte. For measurements, the solution of CT was dissolved in 0.5 M KCl solution whereas CdTe QDs was deposited on a clean electrode as a submonolayer.

**DNA concentration measurements:** The concentration of DNA isolated from *Streptomyces sanglieri* was determined using Thermo Scientific NANODROP 2000 spectrometer.

#### Synthesis:

**Synthesis of water soluble MSA capped CdTe QDs:** MSA capped CdTe QDs were prepared using a facile one-pot approach as reported earlier.<sup>19</sup> In a nutshell, 3mM 20 ml solution of CdCl $_2$ , 0.75 mM 20 ml Na $_2$ TeO $_3$  and 9 mM of MSA were mixed together and then poured into a high capacity buffer (15 mM 10 ml Borax solution and 15 mM 10 ml Citric acid) with further addition of Sodium hydroxide to tune pH 7-7.5. To ensure complete mixing of precursors, the reaction mixture was stirred for 5 min at room temperature followed by addition of NaBH $_4$  for nucleation. Thereafter, the mixture was refluxed at 100 $^\circ$ C upto different time intervals to obtain a size dependent fluorescence emitter covering different

wavelengths of visible spectrum. The formation of MSA capping on QDs surface was confirmed by FTIR measurements (refer Fig. S1, *ESI*).

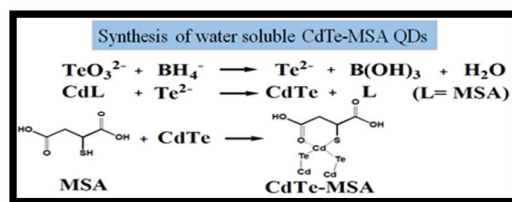


Fig. 1 Synthetic pathway for CdTe/MSA QDs.

**Synthesis of Cationic Curcumin-Tryptophan biohybrid (CT):** Cationic CT was synthesized in three steps:

**Step 1: Fischer Esterification:** Reaction mixture containing Curcumin (0.01M, 3.689 g) and BOC-L-tryptophan (0.02M, 6.09g) was refluxed with a small amount of p-TsOH for 1 hr to produce an equilibrium mixture. Aliquot of the reaction mixture was taken out in ice cold water. The ester formed was collected via simple filtration and the formation of ester has been confirmed by FTIR (refer Fig. S2, *ESI*). The formation of pure ester with NBOC intact has been confirmed by <sup>1</sup>H NMR (refer Fig. S3, *ESI*) and LC-MS (refer Fig. S4, *ESI*).

**Step 2: Microwave assisted deprotection:** The ester formed in step 1 (1 mMol) is mixed with p-TsOH (2 mMol) in a beaker containing 5 ml methanol. It was then exposed to microwave irradiation until the completion of deprotection. On cooling to room temperature, the aminoacid p-TsOH salt was separated as a solid, which was then filtered and washed with methanol. Deprotection of the ester has been confirmed by LC-MS (refer Fig. S5, *ESI*). The zeta potential value of the solution was measured with the help of DLS and it was found to be -14.1 eV (refer Fig. S6, *ESI*).

**Step 3: Protonation:** Protonation of amine of deprotected ester was done by using conventional method employing 0.05 M HCl. This has been supported by measuring the change in the Zeta Potential value which was found to be +6 eV.

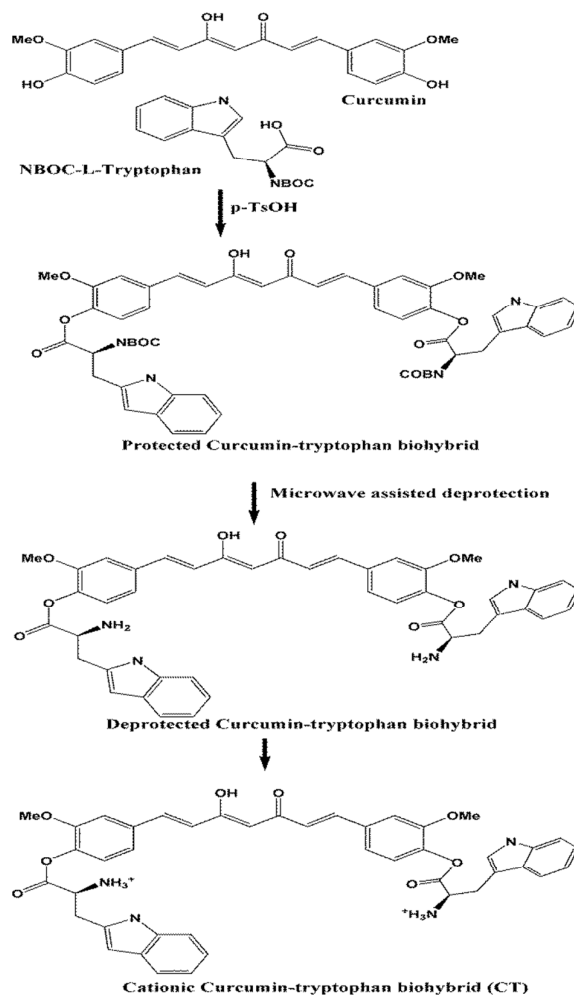


Fig. 2 Reaction scheme for cationic CT synthesis

**Results and discussions:****Characterization of QDs:**

For the synthesis of water soluble CdTe QDs, CdCl<sub>2</sub> and Na<sub>2</sub>Te were used as precursor solutions and MSA as ligands with pH adjusted to 7-7.5. According to an empirical size fitting formula (1), the sizes of 1, 2, 3, 4, 5 and 6 hour samples were calculated<sup>20</sup> as follows:

$$D = (9.8127 \times 10^{-7}) \lambda^3 - (1.7147 \times 10^{-3}) \lambda^2 + (1.0064) \lambda - 194.84 \quad (1)$$

where, D (nm) and  $\lambda$  are respectively the size and wavelength of the excitonic absorption peak of CdTe QDs, the sizes of 1, 2, 3, 4, 5 and 6 hrs samples were estimated as being 3.11 nm, 3.43 nm, 3.62 nm, 3.74 nm, 3.84 nm and 3.97 nm respectively. The size distribution plots of QDs (1hr-7 hrs) as obtained from DLS study was also investigated (refer Fig. S7, *ESI*). PL of 1, 2, 3, 4, 5, 6 and 7 hrs samples were also taken (refer Fig. S8, *ESI*).

First we have utilized the 7 hrs QDs solution synthesized at pH=7.5 and investigated the QD photoluminescence (PL) at various concentration of cationic CT. The high resolution (HR) TEM images presented in (Fig. 3a), illustrate that the QDs are spherically shaped with an average size of 5.6 nm while (Fig. 3b) highlights their lattice fringe and the interplanar spacing was measured to be 0.729 nm, which correspond well to our XRD data. The composition of CdTe QD was qualitatively determined by means of energy disperse X-ray (EDAX) measurements and the relative signals in EDAX, represent the presence of S, Cd and Te elements (refer Fig. S9, *ESI*). The presence of S element includes the S in crystals and MSA capping on the surface of CdTe QDs.<sup>21, 22</sup> The XRD profile of CdTe-MSA QDs as obtained (Fig. 4) shows the presence of peaks at *ca.*  $2\theta = 24^\circ$ ,  $40.2^\circ$  and  $46.6^\circ$  are related to the characteristic (111), (220) and (311) planes of CdTe on the Zinc blend (cubic) crystal structure and the interplanar spacing was found to be 0.69 nm as obtained from Scherrer equation.

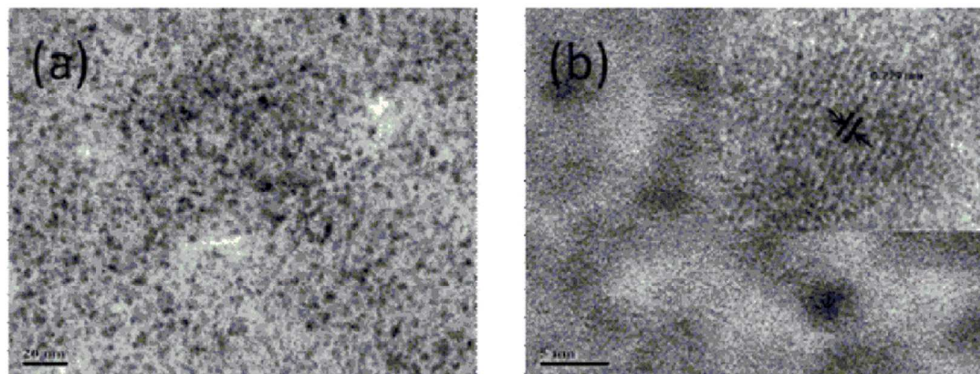


Fig. 3 (a) TEM image (at 20 nm scale bars) of CdTe-MSA prepared by one pot synthesis. (b) HRTEM image (at 5 nm scale bars) lattice fringes of QDs.

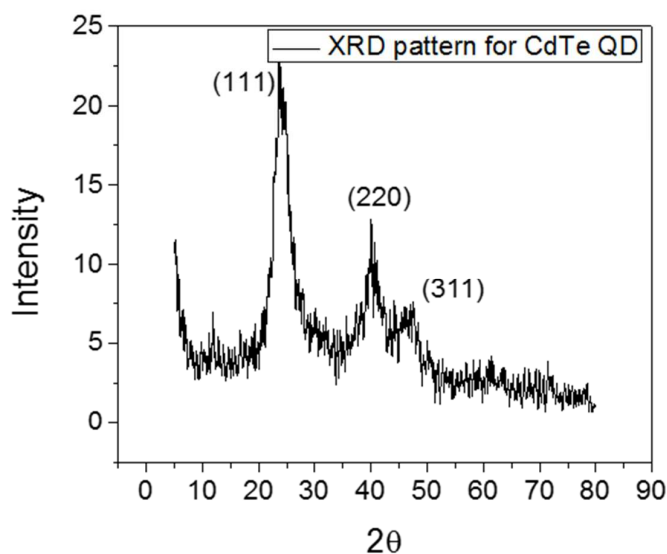


Fig. 4 XRD profile of synthesized CdTe/MSA QDs.

**UV-Vis Study:** UV-Vis spectra was recorded for the synthesized organic counterpart CT and its comparative study was carried out with curcumin and tryptophan (refer Fig. S10, *ESI*).

**PL Study:** The PL intensity of QDs gradually decreases with 99.4% efficiency with incremental addition of cationic CT (0.06 nM to 0.31 nM) (Fig. 5). The regular decrease may be attributed to surface adsorption of cationic CT on the surface of negatively charged QDs. The Stern Volmer plot suggests the probable mechanism behind the quenching (static or dynamic). The upward curvature towards Y-axis is suggestive of dynamic or a mixture of static and dynamic quenching mechanisms (Fig. 6).

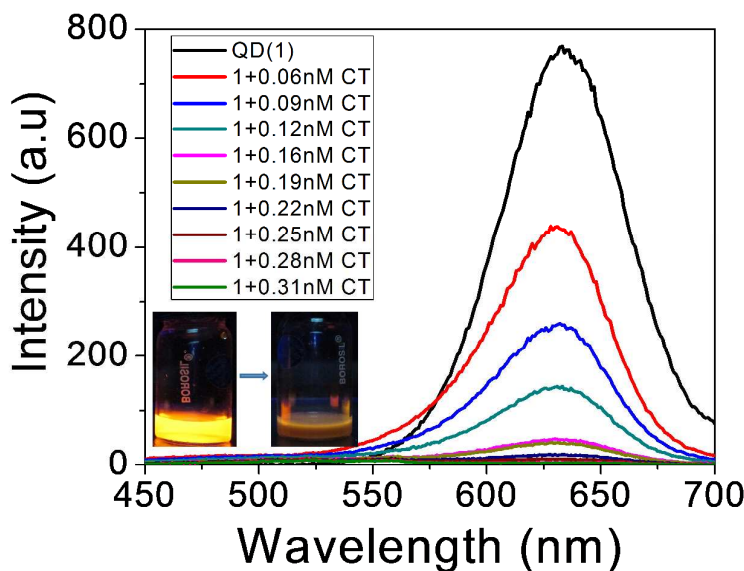


Fig. 5 Fluorescence quenching of CdTe-MSA ( $1 \times 10^{-9}$  M) after addition of cationic CT ( $0.06 \times 10^{-9}$  M to  $0.31 \times 10^{-9}$  M) at pH 7, and  $\lambda_{\text{ex}} = 350$  nm.

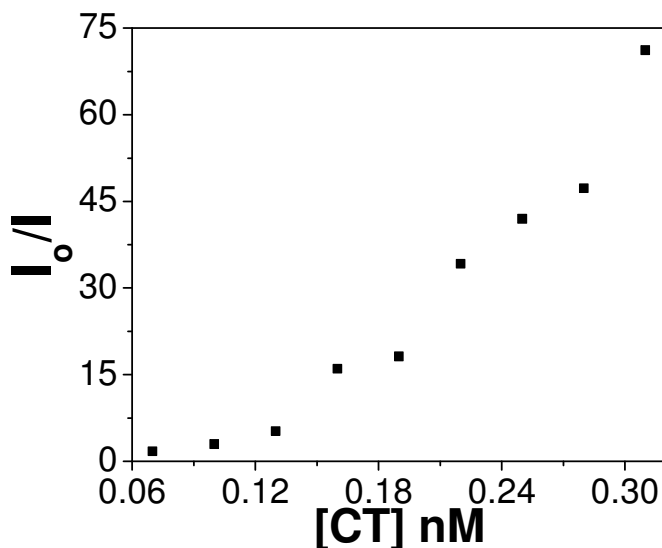


Fig. 6 SV plot of CdTe-MSA with cationic CT showing upward curvature towards Y-axis.

The hybrid system generated by QDs and the macrocyclic systems like CT has wide applications.<sup>23, 24</sup> Here, the quenching has resulted from the formation of nanohybrid. This, nanohybrid has been formed as a result of electrostatic interaction which has been confirmed by NaCl addition to the hybrid system as it results in PL restoration via detachment of cationic CT from QDs (refer Fig. S11, *ESI*).

However, there is no drastic change in peak position upon addition of cationic CT on QDs probably because of restriction of conformational mobility of indole group of Tryptophan moiety. Upon addition of incremental amount of ds DNA into nanobiohybrid QD-CT, restoration of PL intensity was observed with an efficiency of 99.28% for 2734 ng of ds DNA with blue shift (Fig. 7).

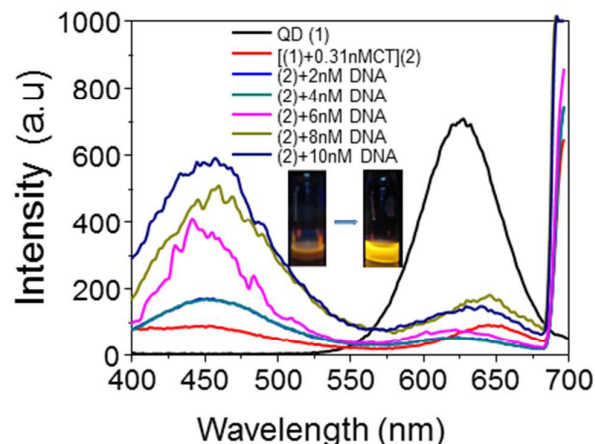


Fig. 7 Fluorescence regain behavior of CdTe-MSA ( $1 \times 10^{-9}$  M) and cationic CT in presence of different concentrations of  $(2-10) \times 10^{-9}$  M ds DNA.

This nanohybrid formation and detachment of QDs was further supported by the change in hydrodynamic radius as observed from DLS study (Fig. 8).

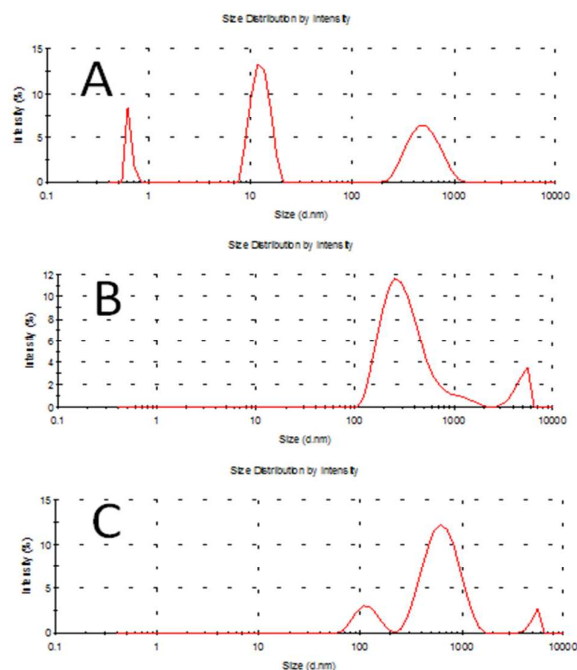


Fig. 8 DLS study depicting average size distribution of A: CdTe-MSA, B: CdTe-MSA + cationic CT and C: CdTe-MSA + cationic CT + ds DNA.

**Mechanistic details:** The sensing strategy is based on electronic switch- firstly fluorescence 'turn off' upon addition of cationic curcumin-tryptophan complex to MSA capped QDs followed by fluorescence 'turn on' upon addition of ds DNA to the nanohybrid so formed. Both the processes are highly efficient with quenching and regain efficiency of almost 100%. Now we delve into the reasons behind such high efficiency. FRET, which is a widely used process is ruled out as the absorption spectrum of acceptor and emission spectrum of donor do not overlap (refer Fig. S12, *ESI*). Here, the quenching has resulted by virtue of Photoinduced Electron Transfer (PET) mechanism. The process starts with initial absorption of a photon by an electron in the ground state as a result of which the electron jumps to the excited state, which then moves to the excited state of curcumin-tryptophan complex forming a charge transfer exiplex (CT exiplex). The exiplex so formed ultimately jumps to the ground state with no emission, which is observed as fluorescence 'turn off'. Also, a size dependent quenching study was carried out and it was found that the quenching effect is more efficient in case of QDs of greater size, which supports the fact that the quenching has resulted from electron transfer and not hole transfer (plots given later). Moreover, thermodynamic feasibility of the process was confirmed with the help of Rehm-Weller equation:

$$\delta G_{e^{-}} = E_{1/2}^{(ox)} - E_{1/2}^{(red)} - E_S + C$$

where,  $E_{1/2}^{(ox)}$  is the oxidation potential of CdTe/MSA QDs,  $E_{1/2}^{(red)}$  is the reduction potential of Curcumin-tryptophan cationic complex,  $E_S$  is the excited state energy of fluorophore, and  $C$  is the coulombic term.<sup>25</sup> The negative  $\delta G_{et}$  value indicates the process is thermodynamically feasible.

Finally, addition of ds DNA to the Charge Transfer complex leads to cleavage of the complex as curcumin-tryptophan hybrid gets intercalated between the two strands of DNA making the QD surface free leading to fluorescence 'turn on'. There are many reported works where derivatives of curcumin have been known to intercalate between the DNA strands.<sup>26</sup> The mechanistic pathway of this process is presented below:

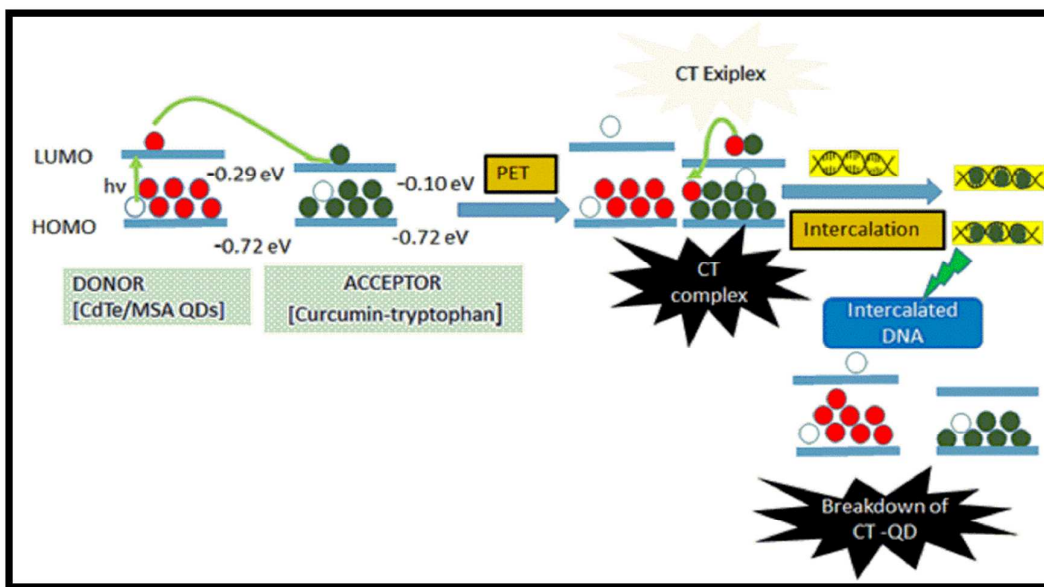


Fig. 9 Mechanistic pathway of electron transfer between CdTe-MSA (donor), cationic CT (acceptor) and subsequent detachment of CdTe-MSA with the intercalation of cationic CT within ds DNA (ds DNA).

To further confirm electron transfer process, a size-dependent quenching effect of QDs PL by cationic curcumin-tryptophan (CT) was investigated,<sup>27</sup> and the corresponding Stern-Volmer plots are presented in the Figure 10. It is found that PL quenching of larger sized QDs (5.6 nm) with increasing CT concentration is more compared to smaller sized QDs (3.4 nm). The  $K_{SV}$  of 5.6 nm QDs is found to be  $9.2 \times 10^{13} \text{ L mol}^{-1}$  while for 3.4 nm QDs, it is found to be  $2 \times 10^{13} \text{ L mol}^{-1}$ . This suggests PL quenching is due to electron transfer mechanism and not hole transfer mechanism.

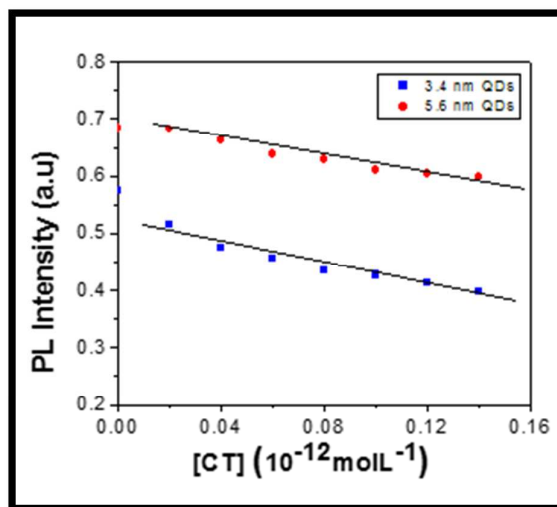


Fig. 10 Comparative SV plots of 3.4 nm QDs and 5.6 nm QDs indicating PL quenching is more for the latter with the addition of cationic CT.

**AFM analysis:** The surface morphology of the sensor system developed was studied in depth with the help of AFM analysis. The two and three dimensional AFM images of the QD, QD+CT and QD+CT+DNA are presented in [Fig. 11 (A, B, C, D, E, F)].

The AFM data provide information regarding size, aggregation and cleavage, which are important phenomena in the present context of our sensor system. The particle and cluster sizes were determined by measuring the Z-axis height.<sup>28</sup> The synthesized QDs exhibit a size in the range (0-15 nm), whereas the nanohybrid formation between QD and CT is justified from the enhancement of size to  $\mu\text{m}$  range (0-3.5  $\mu\text{m}$ ). Moreover, upon addition of DNA to the nanohybrid leads to the formation of new hybrid DNA-CT with the detachment of QDs as it is evident from the change in size (0-600 nm).

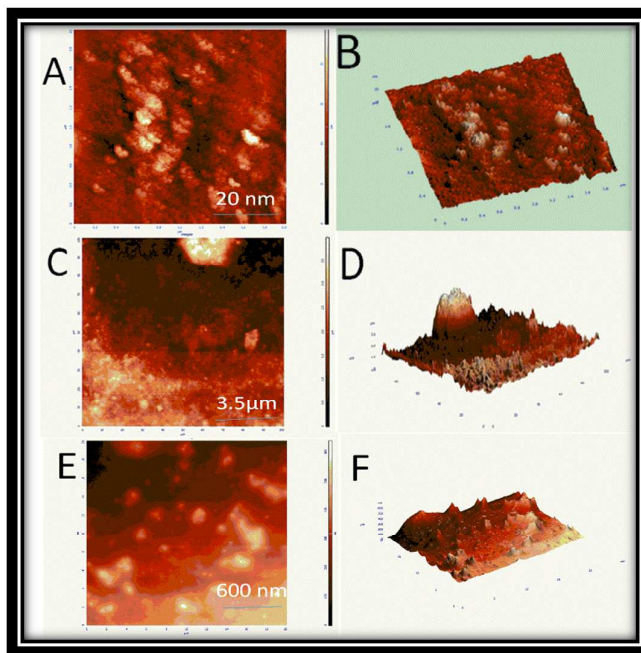


Figure 11 2D and 3D AFM topographic images of A, B: CdTe- MSA, C, D: CdTe-MSA+ cationic CT and E, F: CdTe-MSA+ cationic CT+ ds DNA.

**XRD Analysis:** XRD plots also provide valuable information regarding the sensing strategy. From the XRD plots, it is evident that MSA capped CdTe was formed. Upon addition of CT to CdTe, some crystalline structures were formed along with a broad peak of CdTe, which may be due to the formation of CdTe-CT hybrid, resulting in fluorescence 'turn off'. Further addition of DNA to the hybrid results in cleavage of CdTe with the formation of intercalated DNA with CT as XRD pattern of CdTe+CT+DNA resembles CdTe. This provides evidence regarding detachment of CdTe from the CT+DNA, which leads to fluorescence 'turn on'.

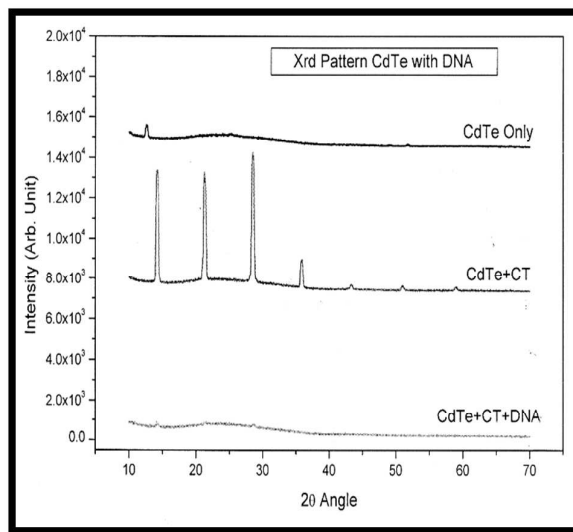


Fig. 12 Comparative XRD plots of MSA capped CdTe, CdTe + CT (cationic) and CdTe + CT (cationic) + DNA.

**Interference study of biomolecules in the CdTe QD-CT nanohybrid:** The interference study of the probe towards ds DNA was further studied by investigating the influence of other negatively charged biomolecules like ss DNA, RNA, primers-1492R and 27F. From the diagram, it can be inferred that such biomolecules have less interference on fluorescence recovery, which indicates that ds DNA is superior in binding with cationic CT. Further the influence of certain vitamins and aminoacids like folic acid (FA), uric acid (UA), aspartic acid (AA), L-cysteine (LC), L-tryptophan (LT) and cobalamin (C) were also investigated. The present system shows minimal interference as depicted in the interference bar diagrams. So, the nanohybrid synthesized is an excellent probe for ds DNA (ds DNA).

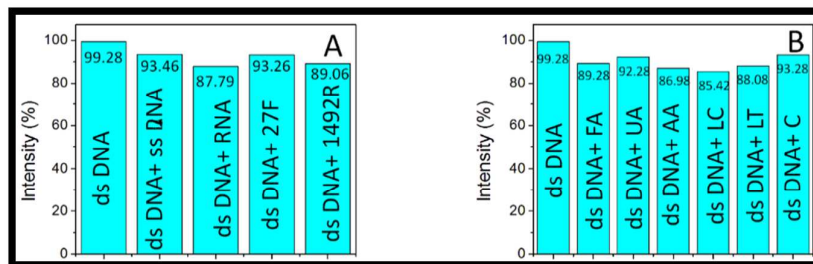


Fig. 13 Bar diagram showing A: Interference study of negatively charged molecules on ds DNA, B: Interference study of aminoacids and certain vitamins on ds DNA.

**Clinical application of the nanohybrid developed as a bacterial DNA sensor:** *Streptomyces sanglieri* is an actinobacteria isolated from soil samples of Pobitora Wildlife Sanctuary (26°12'–26°16'N, 91°58'–92°05'E), Assam, India. The strain was characterized through 16S rDNA sequencing using the 16S ribosomal RNA gene-specific universal primers, 27F 5'-AGA GTT TGA TCC TGG CTC AG-3' and 1492R 5'-GGT TAC CTT GTT ACG ACT T-3'.<sup>23</sup> 16S rDNA sequencing was done in ABI 3130 automated DNA sequencer (Applied Biosystems, USA) and blasted using BlastN for searching the closest match sequence. It produces secondary metabolite-Lactonamycin Z, which has potent antibacterial and antitumor activities.<sup>29</sup> The sensing of bacterial DNA from soil is very important as they develop molecular tool and can bypass cultivation and provide information on the collective soil metagenome.<sup>30-34</sup> The present sensing system provides an efficient platform for sensing such ds DNA.

#### Genomic DNA extraction from *Streptomyces sanglieri*:

Genomic DNA was isolated from *Streptomyces sanglieri*.<sup>35</sup> In a nutshell, *S. sanglieri* was grown in 2 ml GLM broth [Yeast (3g/l), Malt (3g/l), peptone (5g/l) and starch (10g/l); pH 7.4] at 28°C in orbital shaker at 220 rpm for 96 hours. The culture broth was harvested by centrifugation at 8000 rpm for 5 min, washed twice with sterile water and suspended in 0.8 ml lysis buffer (100 mM Tris-HCl, 20 mM EDTA, 250 mM NaCl and 2% SDS and 1 mg/ml lysozyme). 2  $\mu$ L RNase was added and incubated at 37°C for 3 hours with occasional inversion. To this was added 2  $\mu$ L proteinase-K and incubated at 65°C for 30 min. DNA was extracted using phenol, chloroform and isoamyl alcohol (25: 24: 1). The DNA was precipitated by addition of 0.1 volume of 3 M sodium acetate (pH 2) and 2 volume of 96 % ethanol and incubated at -20°C for 60 min. The solution was centrifuged at 12000 rpm for 15 min. The pellet was then washed with 70 % and 90 % ethanol. The pellet was air-dried and suspended in 30  $\mu$ L TE buffer (pH 7.7) and stored at 4°C. The purity of DNA was found to be 1.82.

#### Sensing study of CdTe QD-CT nanohybrid towards bacterial DNA extracted from *Streptomyces sanglieri*

To further study the applicability of the synthesized nanohybrid system QDs-CT towards ds DNA extracted from *Streptomyces sanglieri*, fluorescence titrations were performed with the incremental addition of ds DNA (2  $\mu$ l in each step) to the nanohybrid system (2 ml of the solution). It was found that with the addition of ds DNA, there is regain of fluorescence intensity with blue shift, suggestive of complexation of CT with ds DNA leading to the change in band gap. The fluorescence regain efficiency was found to be 99.38% with the addition of 8 nM of ds DNA. The detection limit was evaluated to be  $1.7 \times 10^{-6}$  M.

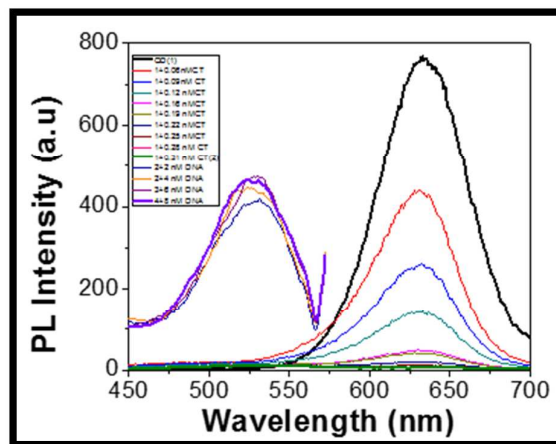


Fig. 14 Fluorescence regain behavior of CdTe-MSA ( $1 \times 10^{-9}$  M) and cationic CT in presence of different concentrations of ds DNA [ $(2-8) \times 10^{-9}$  M] extracted from *Streptomyces sanglieri*

**Comparative study of our system with reported systems:** A comparative analysis was carried out to prove efficiency of our system for ds DNA to other reported systems in this field (Fig. 15). It was found that our system provides better sensitivity range and limit of detection compared to reported systems.

Sl. No.	Hybrid system	Sensitivity range	Limit of Detection
1.	QD- Methylene blue	$1.25 \times 10^{-7}$ - $1.25 \times 10^{-6}$ M	$4.23 \times 10^{-8}$ M
2.	QD- Anticancer drug	$0-16 \times 10^{-6}$ M	
3.	QD- cationic porphyrin	$6.5 \times 10^{-9}$ - $29.6 \times 10^{-9}$ M	$2.72 \times 10^{-9}$ M
4.	QD-1,10-phenanthroline dyads	$0.5 \times 10^{-9}$ - $60 \times 10^{-9}$ M	$3 \times 10^{-9}$ M
5.	QD- Nile blue	$0-25 \mu\text{g ml}^{-1}$	$2.78 \times 10^{-7}$ M ( $2.78 \text{ng ml}^{-1}$ )
6.	QD- Cationic CT	$6 \times 10^{-11}$ - $31 \times 10^{-11}$ M	$1.37 \times 10^{-10}$ M

Fig. 15 Comparative analysis of the present system with reported works in this field (1-5, references- 36, 37, 17, 27, 38 respectively)

**Conclusion:** In a nutshell, we have developed a highly sensitive new sensor with an excellent detection limit based on commercially available cheap biomaterial curcumin for solution based ds DNA molecules detection. This method incorporating inorganic-organic hybrid material as a sensing tool is simple and fast because chemical labelling or modification of the ds DNA is not required. The sensitivity range and the limit of detection of the sensor developed is much higher than the reported hybrid materials in this field. The use of curcumin-tryptophan with CdTe QDs as one type of sensor based on QD-conjugation for DNA sensing and sensing of bacterial DNA isolated from *Streptomyces sanglieri* with our system has been reported here for the first time, which further enhances its applicability. This work will provide a new insight to the use of curcumin for biosensing applications. However, such systems lack high selectivity, portability and biodegradability. Therefore, this work will provide a challenge to the material scientists to design highly selective, more sensitive, portable and regenerable green biosensors for highly specific nucleotide sequence detection both in laboratory and clinical analysis. Such works in future will revolutionize the field of genetic disease diagnosis.

**Acknowledgements:** This work was supported by Department of Science and Technology (DST), Govt. of India. Authors are thankful to Bedanta Gogoi, Sayan Roy Chowdhury and Priyanka Dutta, for their cooperation in this work. CIF, IASST and CIF, IIT Guwahati are also acknowledged. S. C is thankful to DST, Govt. of India for fellowship.

#### References:

- 1 J. Bell, *Nature*, 2011, **429**, 453-456.
- 2 J. B. Lepecq and C. Paoletti, *J. Mol. Biol.*, 1967, **27**, 87-106.
- 3 P. G. Sammes and G. Yahiolu, *Chem. Soc. Rev.*, 1994, **23**, 327-334.
- 4 C. V. Kumar and E. H. Asuncion, *J. Am. Chem. Soc.*, 1993, **115**, 8547-8553.
- 5 Y. Xing and J. Rao, *Cancer Biomarkers*, 2008, **4**, 307-319.
- 6 I. L. Medintz, H. T. Uyeda, E. R. Goldman and H. Mattoussi, *Nature Materials* 2005, **4**, 435-446.
- 7 S. Tyagi and F. R. Kramer, *Nat. Biotechnol.*, 1996, **14**, 303-308.
- 8 P. Zhang, T. Beck and W. Tan, *Angew. Chem., Int. Ed.*, 2001, **40**, 402-405.
- 9 S. Tyagi, S. A. E. Marras and F. R. Kramer, *Nat. Biotechnol.*, 2000, **18**, 91-1196.
- 10 B. Dubertret, M. Calame and A. Libchaber, *J. Nat. Biotechnol.*, 2001, **19**, 365-370.
- 11 R. Haner, S. M. Biner, T. Meng and V. L. Malinovskii, *Angew. Chem., Int. Ed.* 2010, **49**, 1227-1230.
- 12 J. W. J. Li, Y. Z. Chu, B. Y. H. Lee and X. L. S. Xie, *Nucleic Acids Res.*, 2008, **36**, No. e36.
- 13 W. Xu, X. Xue, T. Li, H. Zeng and X. Liu, *Angew. Chem., Int. Ed.*, 2009, **48**, 6849-6852.
- 14 X. Zuo, F. Xia, Y. Xiao and K. W. Plaxco, *J. Am. Chem. Soc.*, 2010, **132**, 1816-1818.
- 15 M. A. Jhonsi and R. Renganathan, *J. Colloid Interface Sci.*, 2010, **344**, 596-602.
- 16 I. Yildiz, M. Tomasulo and F. M. Raymo, *Proc. Natl. Acad. Sci. U. S.A.*, 2006, **103**, 11457-11460.

- 1  
2  
3 17 E. Vaishnavi and R. Renganathan, *Analyst*, 2014, **139**, 225-34.  
4  
5 18 S. Kumar, V. Shukla, S. Tripathi and K. Misra, *Indian Journal of Biotechnology*, 2002, **1**, 158-163.  
6  
7 19 S. Chakraborty, M. Gogoi, E. Kalita and P. Deb, *Int. J. Nanosci.*, 2011, **10**, 1191-119.  
8  
9 20 W. W. Yu, L. Qu, W. Guo and X. Peng, *Chem. Mater.*, 2003, **15**, 2854-2860.  
10  
11 21 R. K. Capek, I. Moreels, K. Lambert, M. De, Q. Zhao, A. Van Tomme, F. Vanhaecke, and Z. Hens, *J. Phys. Chem. C.*,  
12 2010, **114**, 6371-6376.  
13  
14 22 H. Goncalves, C. Mendonca and J. C. E. Da Silva, *J. Fluoresc.*, 2008, **19**, 141-149.  
15  
16 23 S. Moeno, T. Nyokong, *J. Photochem. Photobiol. A.*, 2009, **201**, 228-236.  
17  
18 24 E. L. Zenkevich, T. Blaudeck, A. Milekhin and C. Von Borczyskowski, *Int. J. Spectrosc.*, 2011, **2012**, 1-14.  
19  
20 25 J. R. Lakoweicz, *Principles of Fluorescence Spectroscopy*, 3<sup>rd</sup> Eds, Springer, 1999, Chapter 9, p 334-351.  
21  
22 26 K. E. Erkkila, D. Todom and J. K. Barton, *Chem. Rev.*, 1999, **99**, 2777-2795.  
23  
24 27 L. Zhang, K. Zhu, T. Ding, X. Hu, Q. Sun and C. Xu, *Analyst*, 2013, **138**, 887-893.  
25  
26 28 V. Poderys, M. Matulionyte, A. Selskis and R. Rotomskis, *Nanoscale Res. Lett.*, 2010, **6**, 1-6.  
27  
28 29 S. V. Satheja and S. R. D. Jebakumar, *Journal of Basic Microbiology*, 2011, **51**, 71-79.  
29  
30 30 A. Holtzel, A. Dieter, D. G. Schmid, R. Brown, M. Goodfellow, W. Beil, G. Juno and H. P. Fiedler, *The Journal of*  
31 *Antibiotics*, 2003, **56**, 1058-1061.  
32  
33 31 J. D. Van Elsas, R. Costa, J. Jansson, S. Sjoling, M. Bailey, R. Nalin, T. M. Vogel and L. Van Overbeek, *Trends in*  
34 *Biotechnology*, 2008, **26**, 591-600.  
35  
36 32 J. Ragendhran and P. Gunasekaran, *Biotechnology Advances*, 2008, **26**, 576-590.  
37  
38 33 R. Daniel, *Current option in Biotechnology*, 2004, **15**, 199-204.  
39  
40 34 J. Handelsman, *Microbiology and Molecular Biology Reviews*, 2004, **68**, 669-685.  
41  
42 35 O. O. Babalola, B. M. Kirby, M. Roes-Hill, A. E. Cook, S. C. Cary, S. G. Burton and D. A. Cowan, *Environmental*  
43 *Microbiology*, 2009, **11** (3), 566-576.  
44  
45 36 J. S. Shen, T. Yu, J. W. Xie and Y. B. Jiang, *Phys. Chem. Chem. Phys.*, 2009, **11**, 5062-5069.  
46  
47 37 J. Yuan, W. Guo, X. Yang and E. Wang, *Anal. Chem.*, 2009, **81**, 362-368.  
48  
49 38 Y. Shen, S. Liu, L. Kong, X. Tan, Y. He and J. Yang, *Analyst*, DOI: 10:1039/C4AN01180E.  
50  
51  
52  
53  
54  
55  
56  
57  
58  
59  
60